THE SOFT POTENTIAL IN RESONANT ATOM-SURFACE SCATTERING

J.R. Manson and J.G. Mantovani
Department of Physics and Astronomy
Clemson University
Clemson, SC 29631
U.S.A.

and

G. Armand
Service de Physique des Atomes et des Surfaces
Centre d'Etudes Nucléaires de Saclay
91191 Gif-sur-Yvette CEDEX
FRANCE

ABSTRACT

We consider several aspects of the theory of resonant scattering in low energy atom-surface systems using soft potentials. A method is presented to account for thermal effects in selective adsorption resonances by taking the thermal average of the t-matrix in a decoupling approximation, and comparison is made with experiment. Further calculations indicate that the specular intensity under resonant conditions has a temperature dependent structure which is quite different from that away from resonance. A consideration of the resonant diffraction of 63 meV He atoms by graphite shows that the effects of a soft potential can be as important as thermal attenuation in the manner in which it is commonly introduced into the corrugated hard wall model. A treatment of threshold resonances shows that an emerging beam causes a resonance in all diffracted beams, but for potentials with a soft repulsive part these are too weak to be readily seen in an experiment.

1. INTRODUCTION

In this paper we would like to present the results of several theoretical investigations of atom-surface scattering at low energies using soft potentials. In particular we wish to discuss three different aspects of resonant scattering. By the adjective soft we mean an interaction potential in which the repulsive wall has a finite slope, as opposed to the corrugated hard wall model (CHW). The CHW is an

B. Pullman et al. (eds.), Dynamics on Surfaces, 23–36.

attractive model particularly because of its ease of calculation, but it is clear that even though the real repulsive potential is very strong there is some penetration of the wavefunction into the surface and this has a pronounced effect on the relative diffraction intensities (1). A soft potential is particularly important for scattering by metals where the incoming atoms are reflected several atomic units in front of the surface by the exponential tail of the electron cloud. The need for a soft potential to explain the relative intensities of diffraction peaks from metals has been rather thoroughly discussed elsewhere (2,3). Here, we would like to confine our discussion to resonant processes and how they are affected by the softness of the potential. In Section 2 we consider the effects of thermal attenuation in bound state resonances (selective adsorption) and compare the results with He scattered by a stepped copper surface. Section 3 is a discussion of the selective adsorption resonances of He incident on graphite and we show that a soft repulsive wall can modify the resonance signatures as much or more than thermal effects as commonly introduced into the CHW. In Section 4 we consider the threshold resonance which occurs with the emergence of a previously evanescent diffraction beam. Using the example of H_2 scattered by a Cu(100) surface we show that such resonances will be difficult to observe in realistic situations.

2. THERMAL ATTENUATION AND RESONANT SCATTERING

The selective adsorption resonance occurs when a bound state (or adsorption level) becomes accessible to the incident particle. The opening up of this additional degenerate intermediate state gives rise to a characteristic resonance behavior in which the relative intensities of the backscattered diffracted particles can be strongly affected. Elastic calculations have been able to explain the appearance of minima and maxima in the scattered intensities (4,5). However, the neglect of thermal effects can lead to contradictions with experiment in the line shape of a resonance. Better agreement with experiment has been achieved using complex optical potentials (6), and more recently Hutchison (7) has proposed, using the CHW, a method of applying Debye-Waller factors to the scattering amplitudes to account for thermal effects. We discuss here a method for introducing thermal attenuation by use of Debye-Waller factors in the transition matrix formalism. This differs from the approach of Hutchison in that it is particularly well suited to handle the more realistic soft potentials.

We choose to calculate the diffraction intensities using a transition matrix formalism in which the potential V is divided into a distortion term U and a perturbation v, $V = U + v$. Then the intensity of a beam labelled by the surface reciprocal lattice vector $\underline{G}$ is given by

$$I_G = \left| \delta_{G,0} - \text{im } t_{Gi} / (\hbar^2 \sqrt{k_{iz} k_{Gz}}) \right|^2 \qquad 2.1$$

where k_{Gz} is the perpendicular wavevector and

$$t_{Gi} = v_{Gi} + \sum_{\ell} v_{G\ell}(E_i - E_\ell + i\varepsilon)^{-1} t_{\ell i} \qquad 2.2$$

and v_{pq} are the matrix elements of v taken with respect to eigenstates of U. Near conditions for a resonance, singularities appear in the Green function of eq. (2.2), but these can be avoided by using projection methods in which eq. (2.2) is written as a pair of coupled integral equations, only one of which involves the resonant bound states. For the case of a single isolated bound state we have

$$t_{Gi} = h_{Gi} + h_{Gb}\, h_{bi}/(E_i - E_b - h_{bb}) \qquad 2.3$$

$$h_{pq} = v_{pq} + \sum_{\ell}{}' v_{p\ell}(E_i - E_\ell + i\varepsilon)^{-1} h_{\ell q} \qquad 2.4$$

where Σ' means the summation does not include the resonant bound state. The h_{pq} are calculated by iteration and the diffracted beam intensities of (2.1) can be evaluated using (2.3) even under resonant conditions. These intensities may be written in the form

$$I_G = I_G^0 \left| 1 - ib/(x-i) \right|^2 \qquad 2.5$$

where

$$x = [E_i - E_b - \mathrm{Re}(h_{bb})]/\mathrm{Im}(h_{bb}) \qquad 2.6$$

and

$$b = N_G\, h_{Gb}\, h_{bi} \,/\, [(\delta_{G,0} - iN_G\, h_{Gi})\mathrm{Im}(h_{bb})] \qquad 2.7$$

where $N_G = m/(\hbar^2\sqrt{k_{iz}k_{Gz}})$ is the density of states for perpendicular motion. In a plot of I_G versus incident angle or energy the half width of the resonance structure is $\Gamma = -\mathrm{Im}(h_{bb})$, but the resonance shape is mainly controlled by the value of b. For example if $|\mathrm{Re}(b)| >> |\mathrm{Im}(b)|$ the line shape is a single minimum for $-2 < \mathrm{Re}(b) < 0$ and a maximum otherwise. Asymmetry in the form of a mixed maximum-minimum structure appears when Im(b) is non-negligible.

In an exact approach, the thermal average of t_{Gi} would be used to calculate the diffracted intensities of eq. (2.1). The major approximation in our approach is to decouple all of the scattering amplitudes in eq. (2.3) and thermally average each one separately. Thus we follow Hutchison's method of approximating the thermal average by scaling each amplitude by a Debye-Waller factor. The amplitudes h_{Gi}, h_{Gb} and h_{bi} in (2.3) are thermally attenuated by multiplying them by the factors $\exp(-W_{Gi})$, $\exp(-W_{Gb})$, and $\exp(-W_{bi})$ respectively. The exponent W is given by

$$W_{pq} = \tfrac{1}{2}(\Delta k_z)^2 \langle u_z^2 \rangle \qquad 2.8$$

where $\Delta k_z = k'_{pz} + k'_{qz}$ is the total change in perpendicular momentum calculated in the "Beeby approximation", i.e.

$$(k'_{pz})^2 = k_{pz}^2 + 2mD/\hbar^2 \qquad 2.9$$

The quantity $\langle u_z^2 \rangle$ is the effective average square displacement of a surface atom in the normal direction, and may involve averaging the motions of several atoms.

The scaling method must be modified when applied to the amplitude h_{bb}. From the optical theorem, $t-t^{+} = t^{+}(G^{+}-G^{-})t$ (which applies equally well to the h operator) the imaginary part of h_{bb} may be related to the probability of a transition from the bound state to the continuum. Thus we have

$$\mathrm{Im}(h_{bb}) = -(\hbar/2)w_b \qquad 2.10$$

where w_b is the total transition rate. Dividing w_b by the flux of particles in the bound state, $1/\tau_b$, gives the corresponding probability P_b. The time τ_b is a semiclassical quantity which can be estimated in several ways. For the potential described below we find that the approach useful in nuclear resonance theory, i.e. to relate τ_b to the inverse of the level spacing of the bound states, gives values which agree fairly well with the period of a classical particle moving in the well.

The probability that a bound particle will remain bound is $1-P_b$, and thermal attenuation is expected to decrease this value. Thus the expression that we use is

$$\langle \mathrm{Im}(h_{bb})\rangle = -\hbar[1-(1-P_b)\exp(-2W_{bb})]/(2\tau_b) \qquad 2.11$$

with $P_b = 2\tau_b \mathrm{Im}(h_{bb})/\hbar$. The thermal attenuation factor is $\exp(-2W_{bb})$ instead of $\exp(-W_{bb})$ since $(1-P_b)$ is a probability and not a probability amplitude. Thermal effects on $\mathrm{Re}(h_{bb})$ are ignored since it appears only in eq. (2.6) as a shift in position of the resonance, and it is usually small.

The method of treating thermal attenuation as presented here can now be contrasted with the approach of Hutchison. The energy half-width Γ of the resonance is given by Hutchison as

$$\Gamma = [1-|S(N,N)|] \;/\; [|S(N,N)|\, d\delta_N/dE]$$

where S(N,N) is essentially a scattering amplitude and is scaled by a single Debye-Waller factor $\exp(-W_{NN})$, and δ_N is the phase gained after one period of oscillation in the potential well. In the present paper, Γ is given by $\langle \mathrm{Im}(h_{bb})\rangle$ calculated from eq. (2.11). Clearly both methods show that Γ will increase with temperature. However, the two methods differ in the manner in which thermal effects are introduced into the calculation of Γ.

We have carried out calculations for He at 21 meV scattering from the(113) face of copper, a system for which good experimental data is available (8). As a potential we use a corrugated Morse function

$$V = D[\exp(-2\kappa(z-\phi))/v_o - 2\exp(-\kappa z)] \qquad 2.12$$

where $\kappa = 1.05\text{Å}^{-1}$, D = 6.35 meV, and v_o is the surface average of $\exp(2\kappa\phi)$. The function $\phi(x)$ is the one dimensional corrugation function appropriate to this surface

$$\phi(x) = da_x \cos(2\pi x/a_x) \qquad 2.13$$

where d = 0.016 and a_x = 4.227Å is the lattice constant for the steps. The distorted potential U is taken as the Morse function corresponding to the surface average of (2.12). For evaluating the Debye-Waller factors the value of $\langle u_z^2 \rangle$ was taken from the data of Lapujoulade et al. (9).

Figure 1 shows the three bound states which are observed experimentally in the specular beam when there is a resonance with the (10) evanescent diffraction channel. The purely elastic calculations show narrow maxima rising almost to unity, and this is easily understood since for all three resonances Re(b) < -2 and $|\mathrm{Im}(b)| \ll |\mathrm{Re}(b)|$. Introducing the effects of thermal attenuation changes the signature of each resonance into a broader miniumum. Inclusion of effects of angular dispersion of the incident beam (not shown in Fig. 1) makes the calculated curves substantially less deep and slightly broader, although still not as broad as the experimental curves. The calculated resonances for n = 1,2 appear at incident angles slightly different from experiment because the bound states of the Morse potential differ from those of the true potential.

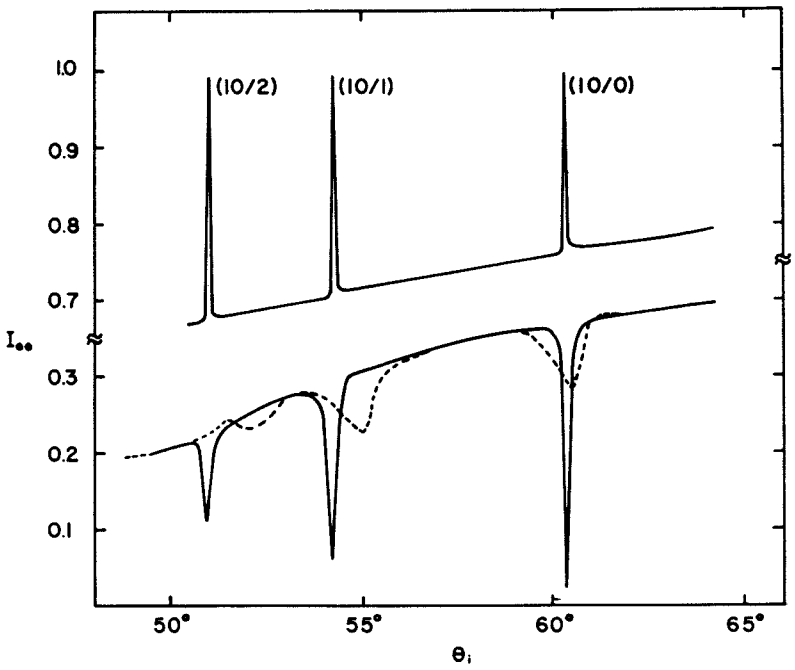

Figure 1. Specular intensity vs. incident angle showing the resonance line shape for He(21meV)-Cu(113). The solid line showing maxima is the elastic calculation, and the solid line with minima is the present theoretical calculation at a temperature of 70 K. Experimental results taken at T = 70 K are shown by the dashed line.

An interesting prediction comes from this work if we examine the temperature dependence of a diffracted beam under exact resonance conditions (i.e. for x=0). In a situation such as that calculated above where $|Re(b)| > |Im(b)|$ the intensity is of the form

$$I_G(T) \cong I_G^0 \exp[-2W_{Gi}(T)] \, [1 + Re\ b(T)]^2 \qquad 2.14$$

where I_G^0 is independent of temperature T. For $Re(b) < -1$ at $T = 0$ and increasing with T, eq. (2.14) shows that $I_G(T)$ will decrease and pass through a minimum at some temperature T_{min} corresponding to $Re(b) \cong -1$. As Re b(T) continues to increase toward zero for $T > T_{min}$ the sum 1 + Re (b(T)) will increase from its minimum value, but this increasing factor is opposed by the term $\exp(-2\ W_{Gi})$ leading to the possibility of a relative maximum at a temperature $T_{max} > T_{min}$. Thus for those resonances, which in a purely elastic calculation have $Re(b) < -1$ and $|Re(b)| >> |Im(b)|$, the intensity measured as a function of temperature will show structure containing both a minimum and a maximum.

The curve marked "a" in Fig. 2 shows the temperature dependence of the minimum point of the (10/0) resonance discussed in Fig. 1. A distinct minimum and a broad maximum are observed. Assuming no angular spread in the incident beam and sufficiently high temperatures, the intensity can be cast in the form

$$I = I^{\circ} e^{-aT} |1+b(t)|^2 \qquad 2.15$$

where $aT = 2W_{Gi}$ and

$$b(T) = b(0)\ P_b \exp(-\alpha T)/[1-(1-P_b)\exp(-\gamma T)] \qquad 2.16$$

with $\alpha T = W_{Gb} + W_{bi} - W_{Gi}$ and $\gamma T = 2W$. For the case at hand α is about an order of magnitude greater than γ. When $|Re(b)| >> |Im(b)|$ the minimum intensity occurs essentially when $b(T) \cong -1$ at the temperature

$$T_{min} \cong (1 + Re[b(0)])/[\gamma(1 - P_b^{-1})] \qquad 2.17$$

A good approximation for T_{max} is

$$T_{max} = P_b[-Re[b(0)]-2+\sqrt{-8Re[b(0)]\gamma/aP_b}]/(2\gamma) \qquad 2.18$$

These simple forms for T_{min} and T_{max} indicate that a measurement of the temperature dependent structure of a resonance can give direct information about the assumed behavior of a particle in the bound state.

Fig. 2 also shows the effect of a simple inclusion of incident angular dispersion on the curve. These calculations indicate that the angular dispersion must be less than 0.1° in order for the minimum structure to be clearly observed. However, even if the angular spread is 0.2° or larger there is still a distinct and characteristic difference between the temperature dependence of the intensity at resonance and away from resonance. Fig. 2 shows that for a large angular spread, the intensity, while monotonically decreasing with T, has a positive

curvature. The experimental Debye-Waller curves which are measured away from resonance give straight lines or negative curvatures.

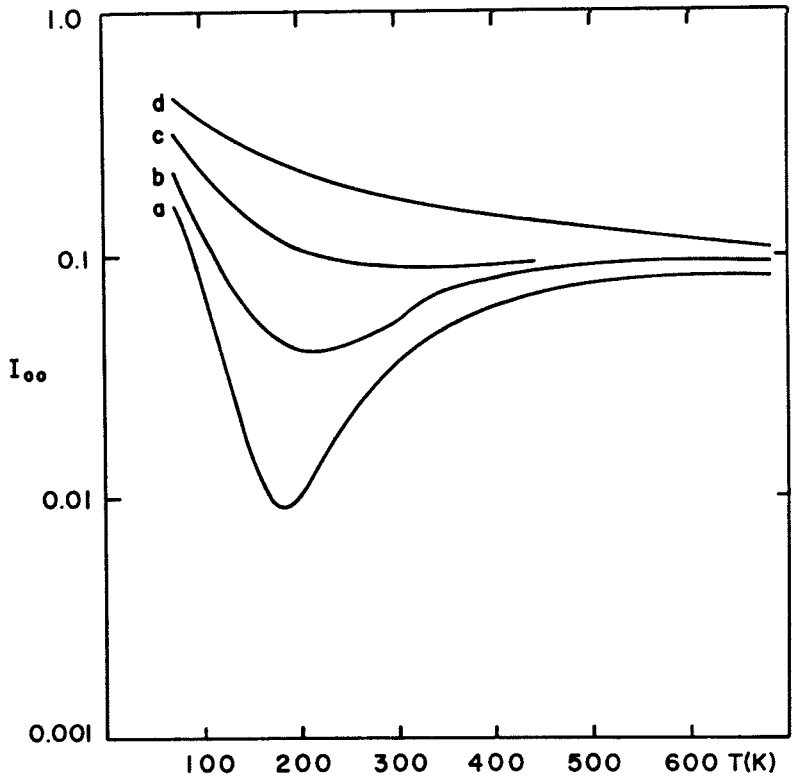

Figure 2. Specular intensity vs. temperature under resonance conditions for the (10/0) resonance of Fig. 1. (a) present theory without angular dispersion, (b) with 0.05° angular dispersion, (c) with 0.1° angular dispersion, and (d) with 0.2° angular dispersion.

3. THE SOFT WALL IN He-GRAPHITE DIFFRACTION

The above section on thermal attenuation in softwall scattering was to a large extent an extension of the earlier work of Hutchison and Celli. Their work is based on the CHW model and was quite successful in explaining the resonance structure for a low energy (21meV) He beam scattered by a graphite surface (7). However, it was later shown that this theory compared rather poorly for the same system when the experiments were done at high energy, 63.8 meV (10). In this section we reconsider the He-Graphite system at the higher energy and show that the effects of using a soft potential, even in a purely elastic calculation, can be of equal or greater importance as the thermal attenuation in the form introduced by Hutchison and Celli.

Again, as in Section 1 we use a transition matrix formalism in which the t-matrix equation of (2.2) is solved by iteration until convergence is obtained. As the potential we again use the corrugated Morse function of eq. (2.12) with parameters $\kappa = 1.31\text{Å}^{-1}$, D = 15.47 meV and a two dimensional corrugation function. In the rectangular coordinates x and y it appears as

$$\phi(x,y) = a\beta_{10}\left[\cos\frac{2\pi x}{a} + 2\cos\frac{\pi x}{a}\cos\frac{2\pi y}{b}\right]$$
$$+ a\beta_{12}\left[\cos\frac{4\pi y}{b} + 2\cos\frac{3\pi x}{a}\cos\frac{2\pi y}{b}\right]$$
$$+ a\beta_{20}\left[\cos\frac{4\pi x}{a} + 2\cos\frac{2\pi x}{a}\cos\frac{4\pi y}{b}\right] \qquad (3.1)$$

with $b = 2.465$ Å, $a = b\cos 30°$, $\beta_{10} = -0.013$, $\beta_{12} = 0.01$ and $\beta_{20} = 0.0$.

The curve marked "A" in Figure 3 shows the experimental data of Cantini et al. for the specular beam in the case in which the (10) evanescent beam is in resonance with the lowest four bound states of the potential. The incident He wavevector is 11.05 $Å^{-1}$ corresponding to 63.8 meV. Curve "B" of Fig. 3 is the present elastic calculation using the Morse potential and the corrugation function of (3.1). Curve "C" is the elastic calculation corrected for the angular spread of the incident beam.

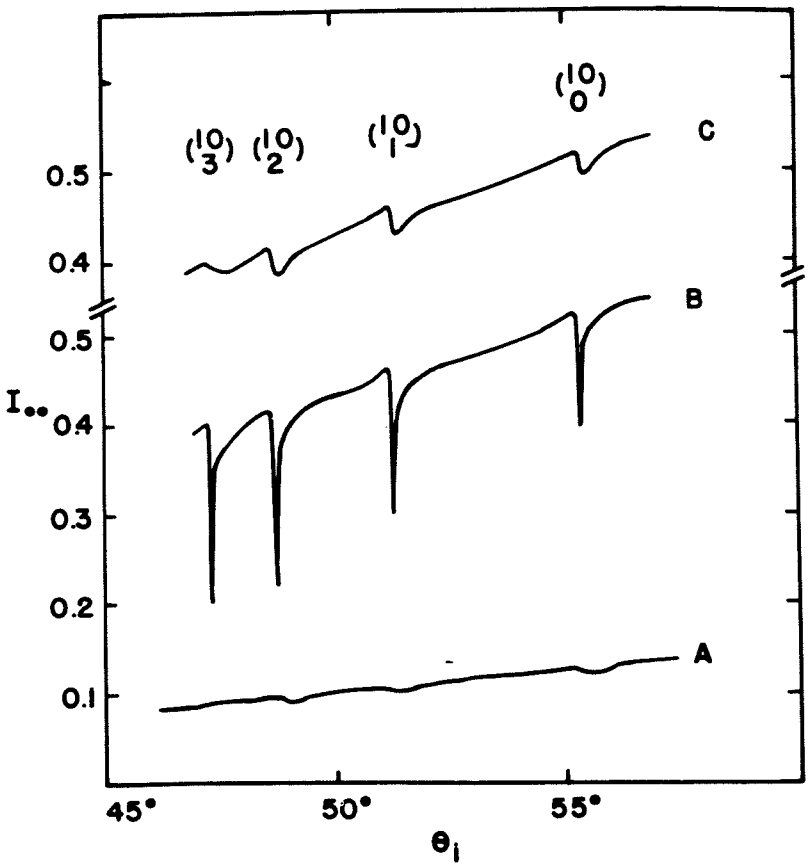

Figure 3. Specular intensity for 63.8 meV He scattered by graphite. (A) experimental data from ref. (10); (B) present elastic calculation; (C) present calculation accounting for angular dispersion of the beam.

Figure 4 gives for comparison the results for the same system reported by Cantini et al. using the CHW, and also the CHW with the Hutchison correction. Clearly, neither the elastic calculation of Fig. 3 nor the Hutchison theory with thermal attenuation agree very well with the very shallow observed resonances. In fact, the best agreement is for the case of the purely elastic softwall calculation corrected for the angular dispersion of the beam. The interesting point is, however, that in comparison with the CHW calculation the present elastic calculation and the Hutchison theory give surprisingly similar results. The Hutchison correction seems to give slightly broader resonance structures, but this is in part an illusion due to the fact that the vertical scale is compressed by the overall Debye-Waller factor which multiplies the curve. This points out that as compared to a CHW calculation, a soft potential can cause changes in resonance intensities which are just as important as the thermal attenuation introduced by the Hutchison method.

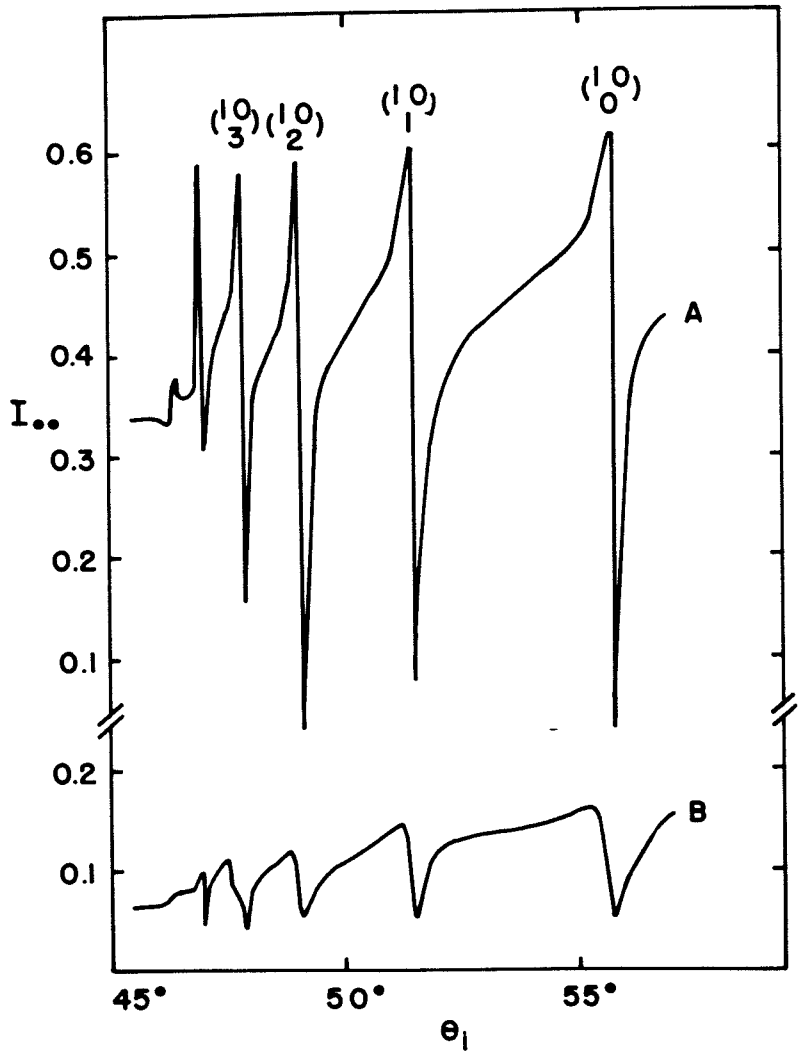

Figure 4. Same system as Fig. 3 (A) CHW calculation, and (B) CHW calculation with thermal attenuation, both from ref. (10).

4. THRESHOLD RESONANCES

In this section we wish to briefly discuss the effects of a soft potential on a completely different type of resonance, that which occurs when an evanescent diffraction beam is just emerging from the surface. These surface threshold resonances, which have been discussed for some time in the context of electron scattering (11,12), have also been suggested as a possible tool for surface investigation with atom scattering (13,14).

The threshold resonance is quite different in character from the selective adsorption resonances discussed above. As explained in more detail below, when a diffraction beam emerges (or disappears) its intensity as a function of incident beam angle grows from zero with an infinite slope. This "sudden" appearance of a new beam causes a rearrangement of the intensities of the other diffracted beams and they too will in general have a singularity in slope at the angle of emergence. A typical example of a calculation is shown in Figure 5 for a model of H_2 scattered at a Cu(100) surface. On the basis of CHW

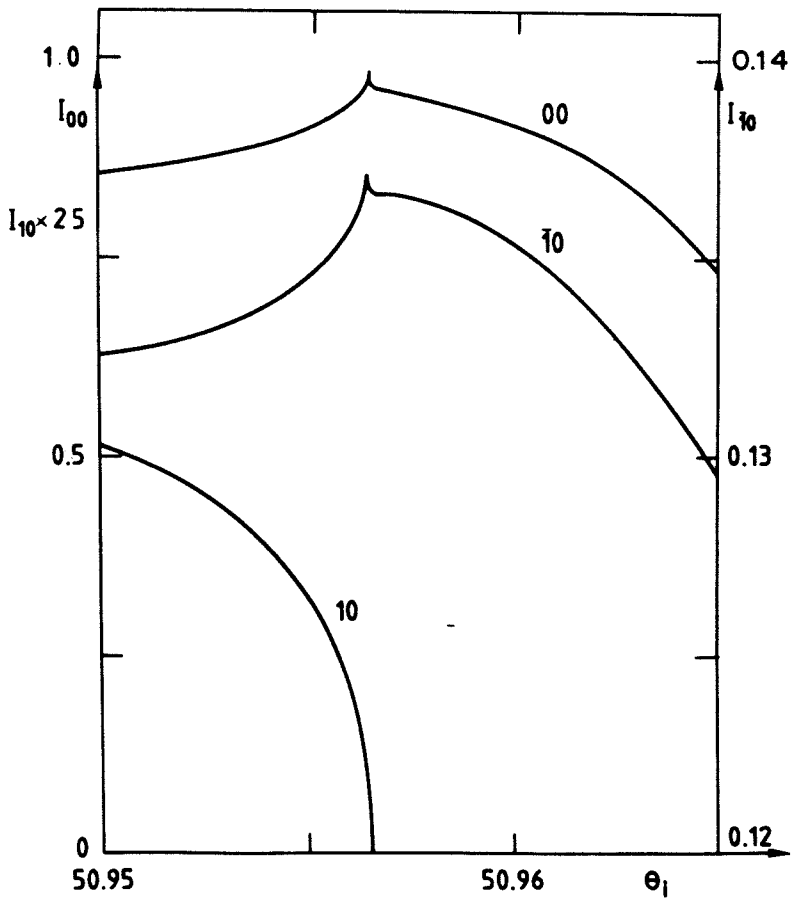

Figure 5. Calculations for H_2 scattered by a Cu(100) surface showing the emergence of the $(\bar{1}0)$ diffracted beam.

calculations it has been suggested that these resonances could be useful in obtaining information on surface structure and particularly on the surface corrugation (13,14). Our calculations using more realistic soft potentials, although confirming this point of view, indicate that the threshold resonance is very sensitive to the slope of the repulsive potential and for all but the very stiffest surfaces will be too weak to be seen in an experiment. Indeed, this conclusion is strengthened by the fact that very few threshold resonances have been clearly identified in the experimental atom-surface scattering literature.

The origin of the threshold resonance is most easily demonstrated as follows. If $\underline{N}$ is the surface reciprocal lattice vector of the emergent beam and I_N its intensity, the slope of interest is

$$\partial I_N/\partial\theta_i = (\partial I_N/\partial k_{Nz})(\partial k_{Nz}/\partial\theta_i) + \ldots \qquad 4.1$$

where the other terms in (4.1) are ignored because they are of no consequence to the discussion. Now since $k_{Nz}^2 = k_i^2 - (\underline{K}_o + \underline{N})^2$ with $\underline{K}_o = \hat{e}\, k_i \sin\sigma$ and $\hat{e}$ a unit vector, we obtain immediately

$$\partial k_{Nz}/\partial\theta_i = -\hat{e}\cdot(\hat{e}\, k_i \sin\theta + \underline{G})\, k_i \cos\theta_i/k_{Nz}, \qquad 4.2$$

the important point being that at emergence when $k_{Nz} \to 0$ this derivative blows up as $1/k_{Nz}$. Thus eq. (4.1) shows that $\partial I_N/\partial\theta_i$ will diverge unless I_N goes to zero at least as fast as k_{Nz}^2 for small k_{Nz}. That this is not the case can be seen be looking at the intensity as a function of the transition matrix (2.1) and examining the form of the matrix elements. From eq. (2.1) we have that the intensity of the emerging beam is

$$I_N = |m\, t_{Ni}/\hbar^2|^2/k_{iz}\, k_{Nz} \qquad 4.3$$

and since $0 \leq I_N \leq 1$ we see that the transition matrix must go to zero at least as fast as $\sqrt{k_{Nz}}$ for small k_{Nz}. However, in general we can argue that $t_{pi} \propto p$ for small p. This is because, from eq. (2.2), t_{pi} will have the same limiting behavior as the matrix element v_{pq} except in highly unusual circumstances, and for all potentials to date which admit to an analytical calculation we find $v_{pq} \to p$ as $p \to 0$. (This includes the corrugated Morse and exponential repulsive potentials as well as the CHW and the simple step potential.) Thus $I_N \to k_{Nz}$ for small k_{Nz} and eqs. (3.2) and (3.1) show that the slope of the intensity curve is divergent. This argument would fail for a case in which the matrix element v_{pq} behaved as $p^{3/2}$ for small p but this appears highly unlikely. In fact, even if one considers a potential with an activation barrier in front of the repulsive potential it is rather straightforward to show that the same linear dependence on p is obtained.

The above arguments justify the statement that the emerging beam appears with an infinite slope in the plot of intensity versus θ_i. Now we need to discuss the other diffracted beams. If we examine $\partial I_G/\partial\theta_i$ where I_G is the intensity of any of the diffracted beams an application of the chain rule for differentiation will produce as one of the terms

$$(\partial I_G/\partial k_{Nz})(\partial k_{Nz}/\partial \theta_i) \qquad 4.4$$

just as in eq. (4.1). If we look closely at I_G of eq. (2.1) and consider it as an infinite summation of terms coming from the expansion of t_{Gi} in the perturbation series, some of these terms for small k_N will be linear in k_{Nz} which will again lead to divergence. Such terms will come from the δ-function (or pole) contribution in the t-matrix equation (2.2), for example we would have

$$t_{Gi} = v_{Gi} - i\pi m v_{GN}\, v_{Ni}/\hbar^2 k_{Nz} + \ldots \qquad 4.5$$

and the second term on the right will have exactly the behavior in k_{Nz} which will lead to a divergence. Thus it is clear that if there is an infinite slope in the emerging diffraction beam, this divergence will also appear in the other diffracted beams except in the unlikely case of a cancellation of all of the divergent terms generated by the perturbation expansion.

It now remains to consider the effects of a soft potential on these resonances. We illustrate this with a model calculation. Since the intensity of the emerging beam at resonance is small we are justified in using the distorted wave Born approximation, $t_{Ni} \cong v_{Ni}$. Choosing the exponential repulsive potential with a corrugation (i.e. the repulsive part of eq. (2.12)) the relevant matrix elements in the limit of small k_{Nz} are

$$v_{Ni} = \lambda_{N0}\sqrt{\pi}\; p_N\; p_i^{\,2}\; \sqrt{p_i \sinh \pi\, p_i}\; /\; (\cosh(\pi p_i)-1) \qquad 4.6$$

where $p_G = k_{\quad}/(2\kappa)$ and λ_{N0} is essentially the Fourier transform of the potential in directions parallel to the surface. Eq. (4.1) for the slope of the emerging intensity becomes

$$\partial I_N/\partial \theta_i = -\pi^3 |\lambda_{No}^2|^2 k_{iz}^4 \hat{e}\cdot(\hat{e}k_i \sin\theta_i \pm N) k_i \cos\theta_i \exp(-\pi k_{iz}/\kappa)/(4\kappa^5 k_{Nz}) \qquad 4.7$$

where we have made the further simplifying assumption that the arguments of the hyperbolic functions are large. For a soft potential (small κ). The behavior of this expression is dominated by the factor $\kappa^{-5}\exp(-\pi k_{iz}/\kappa)$ which is small. Thus for soft potentials the $1/k_{Nz}$ divergence will be very weak and will appear over a very small angular spread.

This is precisely the sort of behavior exhibited by the typical calculation shown in Figure 5 where we consider H_2 scattered at a Cu(100) face. This is an exact calculation using the method of iteration of the transition matrix equation (2.2) until convergence is obtained. The beam is incident in the [110] direction ($\phi_i = 45°$) with a wave vector $k_i = 8.6$ Å^{-1}. The potential parameters are $D = 21.6$ meV, $2\kappa = 1.94$ Å^{-1} and the lattice spacing is 2.55 Å. The corrugation function is

$$\phi(x,y) = (da/2)[\cos(2\pi x/a) + \cos(2\pi y/a)] \qquad 4.8$$

with d = 0.036. The (10) diffraction beam is emergent at an incident angle of slightly less than 50.96°. The steep slope of this curve and the singularity it causes in the slope of the $(\bar{1}0)$ and (00) beams is evident. However, what is important is the scale. The range of angles over which the resonance occurs is so small that it could not be observed with currently available experimental precision. Numerous other calculations tend to confirm the opinion that with a softwall repulsive potential the threshold resonances will be too weak for easy observation (15,16).

5. CONCLUSIONS

We have discussed in this paper three features of resonant scattering using soft potentials and have made the comparison in each case with the corresponding calculations using a hard corrugated wall. Section 2 considers the addition of thermal attenuation in selective adsorption resonances in a manner similar to that introduced by Hutchison and Celli for the CHW. These effects are able to change narrow elastic intensity maxima into broader minima, but the signatures are still not broad enough to agree well with the experimental data for He/Cu(113). An interesting prediction of this work is that the temperature dependence of the diffraction intensity at resonance can have a structure which includes both a maximum and a minimum. This structure is quite different from the behavior away from resonance and if observed could give information about the thermal attenuation of particles trapped in the bound state.

Section 3 is an investigation of selective adsorption resonances for He scattered by graphite and we find that for higher incident energies the effects of a soft potential can be as great as those of thermal attenuation as introduced by Hutchison in the CHW. This implies that the softness of the repulsion cannot be ignored especially at energies where the penetration of the particle wave function into the surface becomes appreciable.

The fourth section is a discussion of threshold resonances generated by soft potentials. We find that the threshold resonance is characterized by a divergence in the slope of the intensity versus θ_i curve, not only for the emerging beam, but for the other diffracted peaks as well. However, we find that the strength of these resonances is strongly dependent on the slope of the potential and for realistic soft potentials they will be difficult to observe.

ACKNOWLEDGEMENTS

We would like to thank J. Lapujoulade, B. Salanon and D. Gorse for many stimulating discussions and C. Manus for his continued support and encouragement. Two of us (JRM and JGM) would like to thank the Service de Physique des Atomes et des Surfaces of the C.E.N. Saclay for its kind hospitality. This work was supported by a NATO Research Grant.

REFERENCES

1. G. Armand and J.R. Manson: Phys. Rev. Lett. 43 (1979) 1839.

2. J. Perreau and J. Lapujoulade: Surf. Sci. 119 (1982) L292.

3. N. Garcia, J.A. Barker, and I.P. Batra: J. Electron. Spectrosc. 29 (1982) L292.

4. H. Chow and E.D. Thompson: Surf. Sci. 54 (1976) 269; K.L. Wolfe and J.H. Weare: Phys. Rev. Lett. 41 (1978) 1663; N. Garcia, V. Celli and F.O. Goodman: Phys. Rev. B 19 (1979) 634; V. Celli, N. Garcia and J. Hutchison: Surf. Sci. 87 (1979) 112.

5. H. Chow and E.D. Thompson: Surf. Sci. 59 (1976) 225; H. Chow: Surf. Sci. 62 (1977) 487.

6. H. Chow and E.D. Thompson: Surf. Sci. 82 (1979) 1; K.L. Wolfe and J.H. Weare: Surf. Sci. 94 (1980) 581.

7. J. Hutchison: Phys. Rev. B 22 (1980) 5671; J. Hutchison, V. Celli, N.R. Hill and M. Haller: Prog. Astronaut. and Aeronautics 74, S.S. Fisher, ed., (1981) 129; V. Celli and D. Evans: Israel J. Chem. 22 (1982) 289.

8. J. Perreau and J. Lapujoulade: Surf. Sci. 122 (1982) 341.

9. J. Lapujoulade, J. Perreau and A. Kara: Surf. Sci. 129 (1983) 59.

10. P. Cantini, S. Terreni and C. Salvo: Surf. Sci. 109 (1981) L491.

11. E.G. McRae: Surf. Sci. 25 (1971) 491.

12. For a recent review see J.C. LeBossé, J. Lopez, C. Gaubert, Y. Gauthier, and R. Baudoing: J. Phys. C15 (1982) 6087.

13. N. Cabrera and J. Solana, in Proc. Intern. School of Phys. "Enrico Fermi", Ed. F.O. Goodman (Compositori, Bologna, 1974) p. 530.

14. N. Garcia and W.A. Schlup, Surf. Sci. 122 (1982) L567.

15. G. Armand: J. Physique 41 (1980) 1475.

16. G. Armand, J. Lapujoulade and Y. Lejay: in Proc. 4th Intern. Conf. on Solid Surfaces, Cannes, 1980, Eds. D.A. Degras and M. Costa [Suppl. to Le Vide, les Couches Minces (1980), p. 587.